Effect of Oxygen on the Belousov−Zhabotinsky Reaction at Low Cerium Concentrations

Anca-Maria Petrascu and Michel H. J. Koch*

European Molecular Biology Laboratory, Hamburg Outstation, Notkestrasse 85, D-22603 Hamburg, Germany

Horst-Dieter Försterling

Fachbereich Physikalische Chemie, Philipps-Universität Marburg, Hans-Meerwein-Strasse, D-35032 Marburg/Lahn, Germany

Received: February 11, 1999; In Final Form: May 11, 1999

An effect of oxygen on the cerium-catalyzed Belousov−Zhabotinsky reaction, which occurs only at low catalyst concentrations and consists of an abrupt drop in the average Ce^{4+} concentration, was investigated. Perturbations of this effect by addition of acrylonitrile or silver nitrate are also described. An attempt was made to model the observations by modifying the Gao−Försterling mechanism (Gao; Försterling. *J. Phys. Chem.* **1995,** *99,* 8638−8644) for the $[Ru(bipy)_3]^{2+}$/bromomalonic acid/bromate system by replacing the ruthenium reactions by those of cerium and adding the reactions of malonic acid in the presence of oxygen. The modified mechanism yields a qualitative interpretation of several important features of the experiments.

Introduction

An effect of oxygen on the cerium-catalyzed Belousov−Zhabotinsky (BZ) reaction[1] consisting in an abrupt drop of the average Ce^{4+} concentration, which is observed only at low catalyst concentrations, was investigated. Although the basic mechanism of the BZ reaction has been understood since the pioneering work of Field, Körös, and Noyes,[2] many of the details of the reaction remain unclear. The effect of oxygen and especially the inhibition of the oscillations were observed early on,[3,4] but the formation of peroxymalonyl radicals in the reaction of cerium with malonic acid in acidic medium was only recently experimentally established.[5] Complex oscillations in the BZ reaction associated with the presence of oxygen were qualitatively described in terms of an Oregonator mechanism.[6] Treindl et al.,[7] who also made an extensive survey of the earlier literature, showed that the nature of the organic substrate influences the effect of oxygen, especially in the autocatalytic oxidation of Ce^{3+} by bromate, and this was attributed to the scavenging of the BrO_2 radicals by malonyl and peroxymalonyl radicals. Although there exists a wealth of mechanisms modeling different features of the dynamics of the BZ reaction under specific conditions, no fully consistent realistic model is yet available.

In an attempt to model our observations, we modified the mechanism of Gao and Försterling[8] for the $[Ru(bipy)_3]^{2+}$/bromomalonic acid/bromate system by replacing the ruthenium reactions by those of cerium and adding the malonic acid reactions[9−11] including those in the presence of oxygen.[5]

This set of reactions qualitatively reproduces the main features of the anaerobic cerium oscillator under our conditions as well as of the effects of oxygen and acrylonitrile. It also yields better simulations of the experimental data in the recent literature.[6]

Experimental Section

The time dependence of the Ce^{4+} concentration was followed at 311 nm on a UVIKON 922 spectrophotometer (Kontron, Neufahrn) thermostated at 30 °C, using standard quartz cuvettes (∼3.5 mL) with an optical path length of 1 cm, equipped with a magnetic stirrer. During the measurements, the cuvettes were closed with a Teflon stopper. Stock solutions in distilled water, unless otherwise specified, were freshly prepared from chemicals purchased from Aldrich, filtered, and degassed with a water pump: 0.23 M $NaBrO_3$, 0.31 M malonic acid (MA), 0.059 M KBr, 2.7 M H_2SO_4, 2.55 mM $Ce(NH_4)_2(NO_3)_6$ in 2.7 M H_2SO_4. For experiments started with Ce^{3+} a 1.275 mM $Ce_2(SO_4)_3$ in 2.7 M H_2SO_4 stock solution was used. The initial conditions for the BZ reaction were 0.07 M $NaBrO_3$, 0.1 M MA, 0.9 M H_2SO_4. When bromide was initially added, the initial concentration was 0.02 M. The cerium concentration was varied between 0 and 0.814 mM. Because of a short delay in starting the recording, the time axis is offset by about 20 s.

The experimental conditions are close to those given in a standard laboratory manual[12] except that a low catalyst concentration was used.

In another set of experiments a dual wavelength (400 and 792 nm) fiber optics spectrophotometer[13] was used with cells of 15 and 150 mL and optical path lengths (d) of 1.9 and 10.8 cm, respectively, through which a gas stream (nitrogen or oxygen) was bubbled. The nitrogen flow was sufficient to provide an inert gas blanket above the solution. The conditions were identical to those above except that MA (Fluka) was further purified by the procedure of Noszticzius et al.[14] and that the Ce^{4+} signal was recorded at 400 nm to compensate for the larger optical path lengths.

Results

The behavior of the cerium oscillator (observed at 311 nm) at different initial Ce^{4+} concentrations in degassed solutions is clearly biphasic below 0.2 mM catalyst, the two phases being separated by a rather sharp drop in the average Ce^{4+} concentration, as illustrated in Figure 1 (top). The parameters used to describe the spectrophotometric signal (i.e., the duration of phase 1 (T''), the period (T), the amplitude (2AC), and the average level (DC) of the signal) are defined in Figure 1 (bottom). Note

* To whom correspondence should be addressed. E-mail: Koch@EMBL-Hamburg.DE. Fax: +49-40-89902 149.

10.1021/jp9905272 CCC: $18.00
Published on Web 08/07/1999

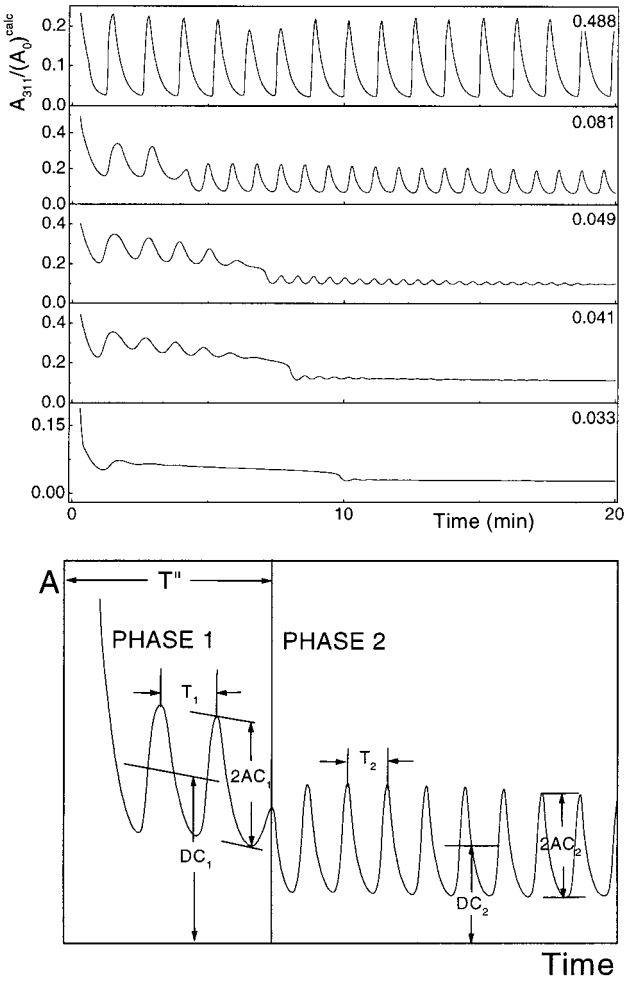

Figure 1. (Top) Behavior of the cerium oscillator (initial concentrations: 0.07 M $NaBrO_3$, 0.1 M malonic acid, 0.02 M KBr, 0.9 M H_2SO_4) monitored by the ratio of A_{311}, the absorbance at 311 nm, and $(A_0)^{calc}$, the absorbance corresponding to the initial Ce^{4+} concentration (mM) indicated on the right of each curve. The solutions were degassed with a water pump. The 3.5 mL cuvette was used with magnetic stirring. (Bottom) Definition of the parameters describing the spectrophotometric signal during the two phases: duration of phase 1 (T''), periods (T_1 and T_2), amplitudes ($2AC_1$ and $2AC_2$), and average Ce^{4+} levels (DC_1 and DC_2) of the signal.

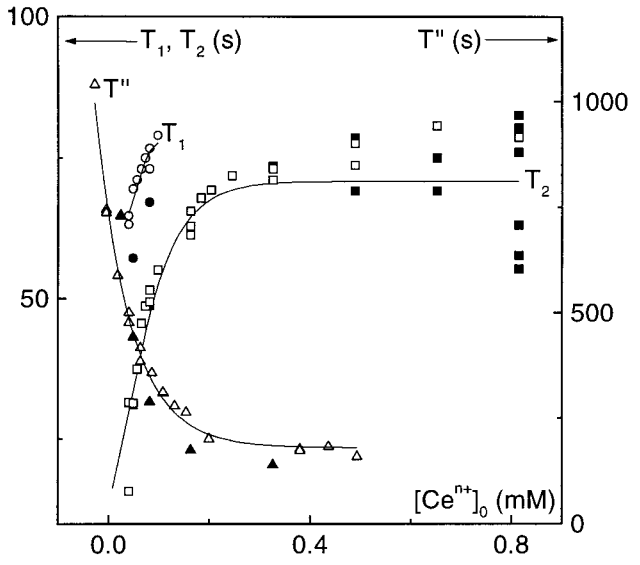

Figure 2. Dependence on the initial Ce^{n+} concentration ($n = 3$ or 4) of the period of the oscillations in phase 1 (T_1; $n = 4$ (○), $n = 3$ (●)) and phase 2 (T_2; $n = 4$ (□), $n = 3$ (■)) and of the duration of phase 1 (T''; $n = 4$ (△), $n = 3$ (▲)).

that, except during the initial decay, the absorbances (≤ 1) remained always in the linear range of the spectrophotometer. The concentration dependence of the parameters is independent of whether the reaction is started with Ce^{3+} or Ce^{4+} as illustrated in Figure 2.

The profile of the oscillations in both phases in Figure 1 (top) evolves from very symmetric maxima at low cerium concentrations to more asymmetric ones at higher concentrations. The profile of the oscillations in phase 1 is always more symmetric than in phase 2.

In each oscillation cycle the time needed for completion of the autocatalytic reaction (reduction of bromate by Ce^{3+}) is nearly constant. The time needed for the completion of the oxidation step (oxidation of (bromo)malonic acid by Ce^{4+}) increases rapidly with increasing Ce^{4+} concentration. In phase 2 the duration of the oxidation step of the oscillations remains constant above $[Ce^{4+}]_0 \cong 0.3$ mM. This is due to the fact that, although the amplitudes (2AC) and the DC levels in both phases increase linearly over the range of cerium concentration used, the amplitude excursions ($2AC_1 = (1.40 \pm 0.18)[Ce^{4+}]_0$ and $2AC_2 = (1.06 \pm 0.02)[Ce^{4+}]_0$ for phases 1 and 2, respectively) increase more rapidly with the initial cerium concentration than the corresponding DC levels $DC_1 = (0.98 \pm 0.07)[Ce^{4+}]_0$, $DC_2 = (0.67 \pm 0.01)[Ce^{4+}]_0$).

Furthermore, the pseudo-first-order rate constant (k_{auto}), determined from the slope of the logarithmic plot ($\ln A$ vs t) for the autocatalytic step of the oscillations, approximated by a pseudo-first-order reaction, increases linearly with $[Ce^{4+}]_0$ in both phases, as expected for an autocatalytic reaction at sufficiently low catalyst concentration, up to an initial cerium concentration of about 0.3 mM, as illustrated in Figure 3. Beyond this initial cerium concentration, k_{auto} levels off (~ 0.3 s^{-1}), but it becomes more difficult to determine the values from the steep slopes. In contrast, the pseudo-first-order rate constant (k_{oxi}) corresponding to the oxidation step in the oscillations is independent, in phase 2, of the initial cerium concentration (~ 0.05 s^{-1}). In phase 1, k_{oxi} increases with $[Ce^{4+}]_0$ up to an initial cerium concentration around 0.3 mM, where phase 1 vanishes. The pseudo-first-order rate constants k_{auto} and k_{oxi} together with the appropriate amplitude excursions (2AC) fully explain the behavior of the oscillation periods T_1 and T_2.

The duration of phase 1 can be shortened by partial removal of oxygen achieved by degassing or by flowing nitrogen (see experimental part for the measurements at 400 nm). The biphasic behavior completely disappears when nitrogen is bubbled through the solutions for about 40 min prior to the addition of catalyst as illustrated in Figure 4. Phase 2 is identical under all conditions. The biphasic character of the BZ reaction using solutions that were not saturated with nitrogen can thus be unambiguously attributed to residual oxygen that is consumed during phase 1. As a further proof, an abrupt increase in Ce^{4+} concentration can be produced when the nitrogen flow is replaced by oxygen flow or by injection of H_2O_2 as illustrated in Figure 5. Attempts to use ammonium persulfate as a source of oxygen radicals failed probably because of stabilization of the persulfate ions at the high sulfuric acid concentrations. Higher oxygen concentrations lead to the well-known inhibition of the oscillations (see Treindl et al.[7] and references therein).

Since oxygen mainly affects the oxidation step of the oscillations, a set of experiments with addition of acrylonitrile was done to obtain more detailed insight into the role of malonyl radical control on the biphasic behavior.

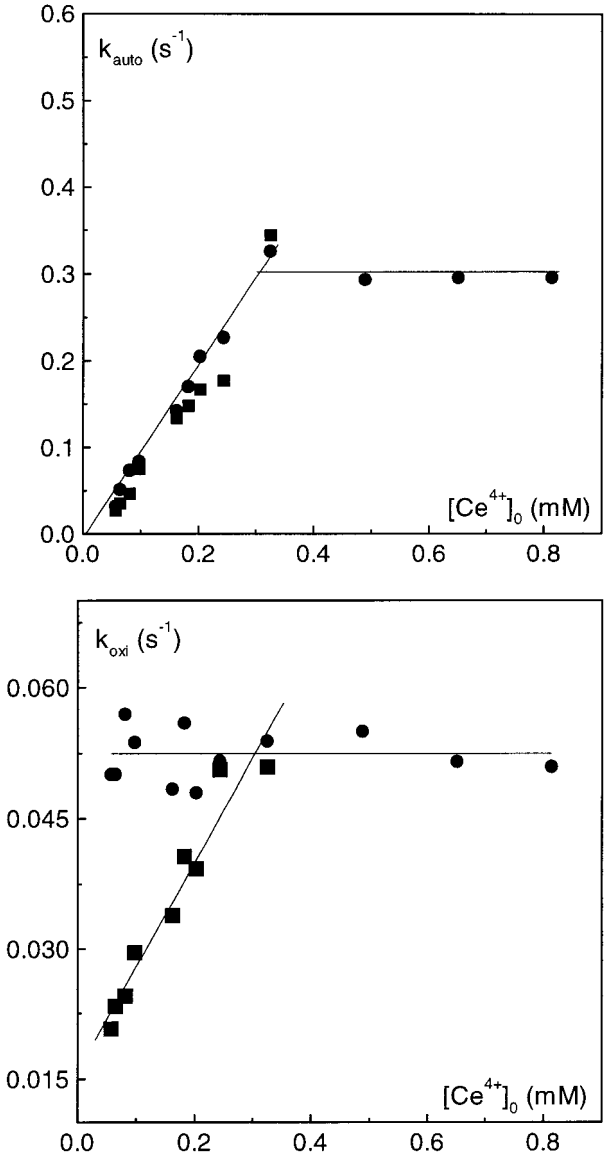

Figure 3. Evolution of the pseudo-first-order rate constants corresponding to the first (k_{auto}) and the second (k_{oxi}) parts of the oscillations as a function of the initial cerium concentration in phase 1 (■) and phase 2 (●) at 30 °C.

The results of the experiments with solutions containing between 0 and 10 mM acrylonitrile, to which the catalyst was added to obtain an initial concentration of 0.073 mM, are illustrated in Figure 6. The interaction between the main radicals in the BZ reaction ($MA^{\bullet}$ and $BrO_2^{\bullet}$) leads to periodic polymerization of acrylonitrile.[15] T_1 slightly increases with acrylonitrile concentration until the oscillations disappear. T'' passes through a minimum at about 1 mM acrylonitrile, and phase 1 gets replaced by a classical induction period with a duration increasing with acrylonitrile concentration. T_2 and DC_2 increase with acrylonitrile concentration, but phase 2 is much less affected than phase 1. The increase in DC_2 level at higher acrylonitrile concentrations is due to light scattering resulting from its polymerization.

These results, and in particular the higher sensitivity of phase 1 to acrylonitrile, indicate that the biphasic behavior is related to the $MA^{\bullet}$ concentration. To verify this, silver nitrate was added and the results are illustrated in Figure 7. Increasing silver nitrate concentrations lead to a progressive increase of the period of the oscillator in phase 1 and an increasingly long induction

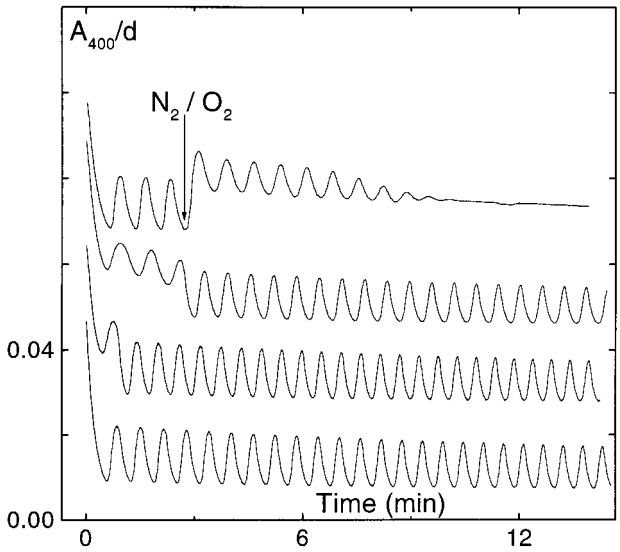

Figure 4. Oscillations in the BZ system after bubbling nitrogen for 40 min (absence of oxygen, bottom), after 20 min degassing (partial removal of oxygen, second curve from bottom), and in normal aerobic conditions (presence of oxygen, second curve from top). The 150 mL cell was used with magnetic stirring. Effect of replacing the nitrogen flow in the anaerobic BZ reaction by an oxygen flow 170 s after the injection of catalyst is shown at the top. The 15 mL cell was used with gas flow stirring. The curves have been displaced vertically for better visualization. Initial Ce^{4+} concentration was 0.076 mM. Other initial concentrations were 0.07 M $NaBrO_3$, 0.1 M malonic acid, 0.02 M KBr, 0.9 M H_2SO_4. A_{400}/d is the absorbance at 400 nm normalized to the thickness of the cell (d).

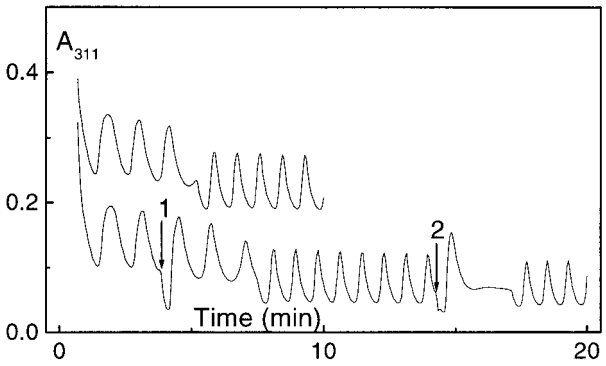

Figure 5. Effect of H_2O_2 injections on the biphasic BZ reaction (0.07 M $NaBrO_3$, 0.1 M malonic acid, 0.02 M KBr, 0.9 M H_2SO_4) at an initial Ce^{4+} concentration of 0.08 mM. Top: reference in the absence of H_2O_2 (displaced vertically). Bottom: injections during phase 1 and phase 2 as indicated by the arrows at initial H_2O_2 concentrations of 0.09 mM (1) and 0.08 mM (2). The solutions were degassed with a water pump. The 3.5 mL cuvette was used with magnetic stirring. A_{311} is the absorbance at 311 nm.

period with a small undershoot in Ce^{4+} concentration in the early part of the curve at the higher $AgNO_3$ concentrations. Significant effects of the silver nitrate on phase 2 are only observed at concentrations above 5×10^{-3} mM $AgNO_3$.

In absence of initially added bromide in the presence of $AgNO_3$ there is a somewhat smaller drop and the initial part of the curve is a smooth decay without undershoot in Ce^{4+} concentration. The difference in the initial decay in the curves is due to the fact that there is no contribution to the absorbance from residual bromine in the absence of initially added bromide. It should also be noted that the Ce^{4+} concentration remains higher, throughout the period of observation, than in the case where bromide is initially added. These observations suggest that the drop in $[Ce^{4+}]$, which under other conditions is

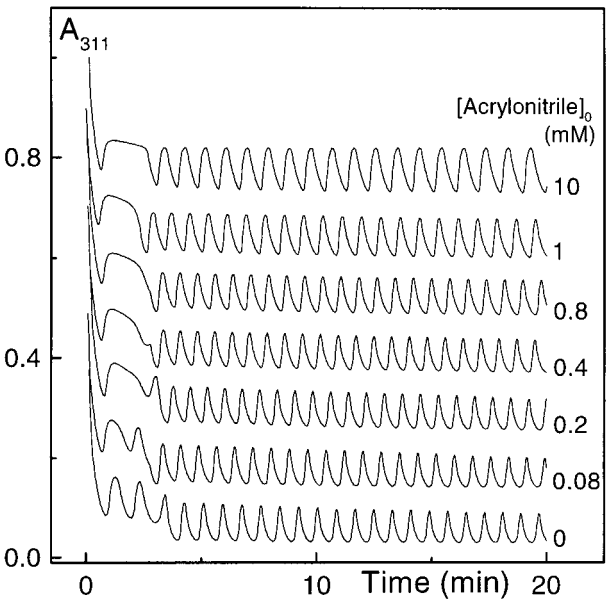

Figure 6. Effect of acrylonitrile on the time course of the Ce^{4+} concentrations (A_{311}, absorbance at 311 nm) in the biphasic BZ reaction at the initial concentrations indicated for each curve. Initial Ce^{4+} concentration was 0.073 mM. Other initial concentrations were 0.07 M $NaBrO_3$, 0.1 M malonic acid, 0.02 M KBr, 0.9 M H_2SO_4. The solutions were degassed with a water pump. The 3.5 mL cuvette was used with magnetic stirring. The curves have been displaced vertically for better visualization.

associated with the biphasic oscillatory behavior, is independent of reactions involving bromide.

Since only a smooth exponential decay without drop is observed when Ce^{4+} is injected in a 0.1 M MA solution in 0.9 M H_2SO_4, it can be concluded that the drop in Ce^{4+} concentration is also associated with reactions involving not only malonyl radicals, as indicated above, but also bromate and of course cerium.

Simulations

The effect of an added compound, oxygen in the present case, on a set of reactions can be formally accounted for either by modifying the rate constants of some of the reactions or by explicitly introducing reactions of the added compound with components of the unperturbed system. The first approach was used to simulate the behavior of the cerium oscillator and its complex oscillations under aerobic conditions.[6] Introduction of this Oregonator model into the GEPASI program,[16] which we used for all simulations, perfectly reproduced the numerical results[6] but failed to reproduce our experimental data even qualitatively, even when the Ce^{3+} reactions were explicitly taken into account. Similarly, the 7-variable mass-action model[10] derived from the 11-variable GRF (Györgyi, Rempe, Field) model[11] failed to produce any oscillations under the conditions of our experiments.

GaF-MA Model. In view of the previous results it was attempted to set up a more realistic model that would also integrate the present knowledge about the BZ mechanism. The set of reactions in this model, referred to as the GaF-MA model, is given in Table 1 and the H^+ concentration for 1 M H_2SO_4 solutions is kept constant at 1.29 M.[17] Note that all reactions of the original FKN model except one ($BrO_2^\bullet + Ce^{4+} \rightarrow BrO_3^- + Ce^{3+} + 2H^+$), which was shown not to occur,[18] appear in the GaF-MA model either in the original or in an updated form.

The GaF-MA model was obtained by modifying the GaF (Gao−Försterling) mechanism, which provides a consistent

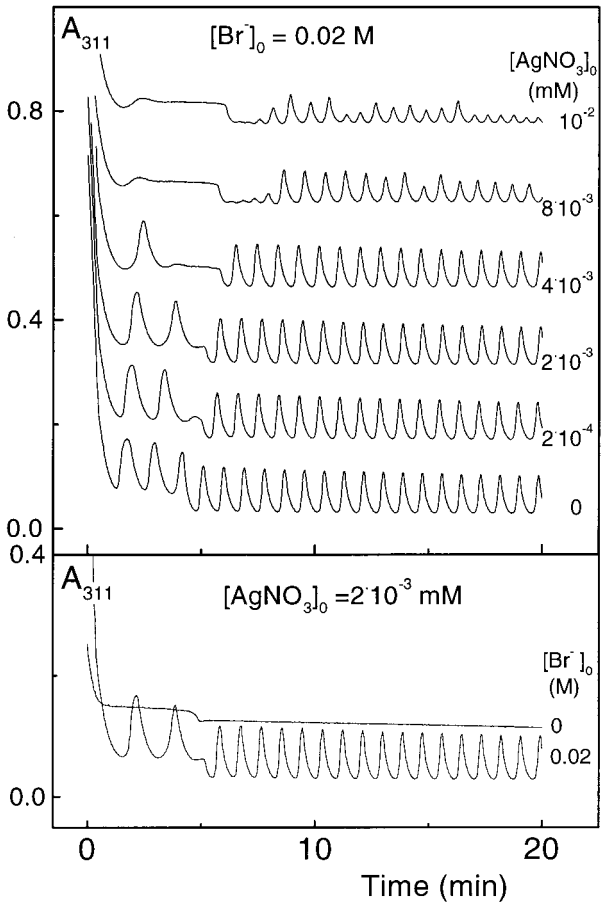

Figure 7. (Top) Effect of $AgNO_3$ on the time course of the Ce^{4+} concentrations (A_{311}, absorbance at 311 nm) in the biphasic BZ reaction at different initial concentrations as indicated on the curves, in the presence of 0.02 M initially added bromide. The curves have been displaced vertically for better visualization. (Bottom) Comparison of the Ce^{4+} level for the same experiment in the presence of 2×10^{-3} mM $AgNO_3$ and in the presence and absence of initially added bromide as indicated on the curves. Initial Ce^{4+} concentration was 0.081 mM. Other initial concentrations were 0.07 M $NaBrO_3$, 0.1 M malonic acid, 0.9 M H_2SO_4. The solutions were degassed with a water pump. The 3.5 mL cuvette was used with magnetic stirring.

model of the $[Ru(bipy)_3]^{2+}$/BrMA/BrO_3^- system.[8] For this purpose, the ruthenium reactions were first replaced by the corresponding cerium reactions, taking into account that the reduced catalyst/$BrO_2^\bullet$ reaction is irreversible for ruthenium but reversible for cerium, whereas the oxidized catalyst/BrMA reaction is reversible for ruthenium and irreversible for cerium.

The GaF model with these modifications was found to work[19] for the cerium/BrMA/bromate system using slightly different values for two of the rate constants in Table 1: $k_{15} = 6.0 \times 10^4$ M^{-2} s^{-1} and $k_{19} = 0.12$ M^{-1} s^{-1}.

In the next step the MA reactions were added to the model. These reactions were put in a form very similar to the BrMA reactions in the GaF model, most of them being written in pairs (e.g., the MA-BrMA pairs R17 (reversible) and R19 (irreversible), R20 and R24, R21 and R25, R22 and R26, R31 and R32, R28 and R29, R34 and R35b). Bromination of MA, for example, was represented by a group of reactions involving the enol (R20 and R22) rather than through a global reaction as is often done. The reaction of MA with HOBr (R23) was written to occur directly, not via the enolized form like for BrMA (R27). Replacing reaction R23 by the corresponding enol reaction (MAEN + HOBr → BrMA + H_2O, $k = 6.7 \times 10^5$ M^{-1} s^{-1})[20] has no influence on the dynamic behavior of the system.

TABLE 1: GaF-MA Model (R1−R34, R35a, R35b) for the Anaerobic Cerium Oscillator and the GaF-MA-N Model (R1−R39) Used To Simulate the Oxygen Effect[a]

no.	reaction	experimental rate constant	model, ref no.	other rate constant, ref no.
1	$Br^- + HOBr + H^+ \rightarrow Br_2 + H_2O$	$8.0 \times 10^9\ M^{-2}\ s^{-1}$	GaF, 8	
2	$Br_2 + H_2O \rightarrow Br^- + HOBr + H^+$	$1.45\ M^{-1}\ s^{-1}$	GaF, 8	
3	$Br^- + HBrO_2 + H^+ \rightarrow 2HOBr$	$2.5 \times 10^6\ M^{-2}\ s^{-1}$	GaF, 8	
4	$2HOBr \rightarrow Br^- + HBrO_2 + H^+$	$2.0 \times 10^{-5}\ M^{-1}\ s^{-1}$	GaF, 8	
5	$Br^- + BrO_3^- + 2H^+ \rightarrow HOBr + HBrO_2$	$1.2\ M^{-3}\ s^{-1}$	GaF, 8	
6	$HOBr + HBrO_2 \rightarrow Br^- + BrO_3^- + 2H^+$	$3.2\ M^{-1}\ s^{-1}$	GaF, 8	
7	$HBrO_2 + H^+ \rightarrow H_2BrO_2^+$	$2.0 \times 10^6\ M^{-1}\ s^{-1}$	GaF, 17	
8	$H_2BrO_2^+ \rightarrow HBrO_2 + H^+$	$1.0 \times 10^8\ s^{-1}$	GaF, 17	
9	$HBrO_2 + H_2BrO_2^+ \rightarrow HOBr + BrO_3^- + 2H^+$	$1.7 \times 10^5\ M^{-1}\ s^{-1}$	GaF, 8	
10	$HBrO_2 + BrO_3^- + H^+ \rightarrow Br_2O_4 + H_2O$	$48\ M^{-2}\ s^{-1}$	GaF, 8	
11	$Br_2O_4 + H_2O \rightarrow HBrO_2 + BrO_3^- + H^+$	$58.18\ M^{-1}\ s^{-1}$	GaF, 8	
12	$Br_2O_4 \rightarrow 2BrO_2^\bullet$	$7.5 \times 10^4\ s^{-1}$	GaF, 8	
13	$2BrO_2^\bullet \rightarrow Br_2O_4$	$1.4 \times 10^9\ M^{-1}\ s^{-1}$	GaF, 8	
14	$2BrO_3^- + 2H^+ \rightarrow HBrO_2 + HBrO_4$	$7.0 \times 10^{-7}\ M^{-3}s^{-1}$	GaF, 8	
15	$Ce^{3+} + BrO_2^\bullet + H^+ \rightarrow Ce^{4+} + HBrO_2$	$6.2 \times 10^4\ M^{-2}\ s^{-1}$	GaF, 24	
16	$Ce^{4+} + HBrO_2 \rightarrow Ce^{3+} + BrO_2^\bullet + H^+$	$1.2 \times 10^4\ M^{-1}\ s^1$	GaF, 17	$7.0 \times 10^3\ M^{-1}\ s^1$, 9−11
17	$Ce^{4+} + MA \rightarrow Ce^{3+} + MA^\bullet + H^+$	$2.3 \times 10^{-1}\ M^{-1}\ s^{-1}$	MA, 9, 29	
18	$Ce^{3+} + MA^\bullet + H^+ \rightarrow Ce^{4+} + MA$	$1.7 \times 10^4\ M^{-2}\ s^{-1}$	MA, 9	
19	$Ce^{4+} + BrMA \rightarrow Ce^{3+} + BrMA^\bullet + H^+$	$0.09M^{-1}\ s^{-1}$	(GaF), 23, 30	$0.4\ M^{-1}\ s^{-1}$,[b]
20	$MA \rightarrow MAEN$	$3.0 \times 10^{-3}\ s^{-1}$	MA, 9, 31	
21	$MAEN \rightarrow MA$	$2.0 \times 10^2\ s^{-1}$	MA, 9, 31	
22	$MAEN + Br_2 \rightarrow BrMA + Br^- + H^+$	$1.91 \times 10^6\ M^{-1}\ s^{-1}$	MA, 9, 31	
23	$MA + HOBr \rightarrow BrMA + H_2O$	$8.2\ M^{-1}\ s^{-1}$	MA, 9	
24	$BrMA \rightarrow BrMAEN$	$1.2 \times 10^{-2}\ s^{-1}$	GaF, 8, 31	
25	$BrMAEN \rightarrow BrMA$	$8.0 \times 10^2\ s^{-1}$	GaF, 8, 31	
26	$BrMAEN + Br_2 \rightarrow Br_2MA + Br^- + H^+$	$3.5 \times 10^6\ M^{-1}\ s^{-1}$	GaF, 8, 31	
27	$BrMAEN + HOBr \rightarrow Br_2MA + H_2O$	$6.6 \times 10^4\ M^{-1}\ s^{-1}$	GaF, 8, 31	
28	$MA^\bullet + MA^\bullet \rightarrow ETA$	$1.0 \times 10^8\ M^{-1}\ s^{-1}$	MA, 20, 21, 32	$4.2 \times 10^8\ M^{-1}\ s^{-1}$, 5
29	$2BrMA^\bullet + H_2O \rightarrow BrMA + BrTA$	$1.81 \times 10^6\ M^{-2}\ s^{-1}$	GaF, 8, 23	
30	$BrTA \rightarrow MOA + Br^- + H^+$	$1.5\ s^{-1}$	GaF, 8	
31	$MA^\bullet + BrO_2^\bullet \rightarrow BrO_2MA$	$5.0 \times 10^9\ M^{-1}\ s^{-1}$	MA, 9	
32	$BrMA^\bullet + BrO_2^\bullet \rightarrow PROD$	$4.0 \times 10^9\ M^{-1}\ s^{-1}$	GaF, 8	
33	$PROD \rightarrow Br^- + P + H^+$	$6.2 \times 10^{-1}\ s^{-1}$	GaF, 8	
34	$PROD \rightarrow HBrO_2 + BrTA$	$4.6 \times 10^{-1}\ s^{-1}$	GaF, 8	
35a	$BrO_2MA \rightarrow GOA + HOBr + CO_2$	$1\ s^{-1}$	MA, 24, 25	
35b	$BrO_2MA \rightarrow TA + HBrO_2$	$1\ s^{-1}$	MA, 24, 25	
35	$MA^\bullet + O_2 \rightarrow MAOO^\bullet$	$1.7 \times 10^7\ M^{-1}\ s^{-1}$	N, 5	
36	$MAOO^\bullet + MA \rightarrow MA^\bullet + MAOOH$	$3.0 \times 10^2\ M^{-1}\ s^{-1}$	N, 5	
37	$Ce^{4+} + MAOOH \rightarrow Ce^{3+} + MAOO^\bullet + H^+$	$2.5 \times 10^3\ M^{-1}\ s^{-1}$	N, 5	
38	$MAOO^\bullet + MAOO^\bullet \rightarrow TA + MOA + O_2$	$2.2 \times 10^8\ M^{-1}\ s^{-1}$	N, 5	
39	$MAOOH \rightarrow P$	$7.0 \times 10^{-2}\ s^{-1}$	N, 5	
40	$O_{2gas} \rightarrow O_2$	$8.33 \times 10^{-5}\ s^{-1}$	Wang conditions, 6	$9.0 \times 10^{-5}\ s^{-1}$,[b]
41a	$MA^\bullet + X \rightarrow MAX$		acrylonitrile effect	$1.0 \times 10^9\ M^{-1}\ s^{-1}$,[b]
41b	$MAX + X \rightarrow MAXX$		acrylonitrile effect	$1.0 \times 10^9\ M^{-1}\ s^{-1}$,[b]

[a] Additional reactions are needed to simulate the aerobic conditions in Wang et al.[6] (R40) or the effect of acrylonitrile (R41a, R41b). $[H_2O] = 55$ M must be explicitly taken into account in GEPASI.[16] MA = $CH_2(COOH)_2$ (malonic acid), MA$^\bullet$ = $^\bullet CH(COOH)_2$ (malonyl radical), BrMA = $BrCH(COOH)_2$ (bromomalonic acid), BrMA$^\bullet$ = $^\bullet CBr(COOH)_2$ (bromomalonyl radical), Br_2MA = $CBr_2(COOH)_2$ (dibromomalonic acid), MAEN = $(HOOC)CHC(OH)_2$ (enolized MA), BrMAEN = $(HOOC)CBrC(OH)_2$ (enolized BrMA), TA = $HCOH(COOH)_2$ (tartronic acid), BrTA = $BrCOH(COOH)_2$ (bromotartronic acid), ETA = $(HOOC)_2CHCH(COOH)_2$ (1,1,2,2-ethanetetracarboxylic acid), BrO_2MA = $OBrOCH(COOH)_2$, MOA = $CO(COOH)_2$ (mesoxalic acid), GOA = OCH(COOH) (glyoxylic acid), MAOO$^\bullet$ = $^\bullet OOCH(COOH)2$ (peroxymalonyl radical), MAOOH = $HOOCH(COOH)_2$ (peroxymalonic acid). [b] Adjusted or optimized in this work.

Reactions R30 and R33 for BrMA illustrate the dominating role of BrMA (BrMA$^\bullet$) in Br^- production.

For R28 only the ETA but not the MAMA (monomalonyl malonate) pathway[21] was taken into account, but this has no effect on our simulations.

The radical transfer reaction between MA$^\bullet$ and BrMA, an important source of bromide ions and crucial for the onset of the oscillations in the GTF model,[9] was not taken into account because ESR and bromide stoichiometry experiments have shown that this reaction can be neglected.[22]

The most recent HPLC results[23] indicating that the recombination of two BrMA radicals (R29) does not lead to BrTA and MOA but first to bromoethenetricarboxylic acid; CO_2 and HBr were also not included in the model. As it is still unclear whether BrTA appears as an intermediate in R34, the latter was left unchanged.

In its final version the GaF-MA model thus contains 36 reactions with 30 dynamic variables of which three were, unless otherwise stated, kept constant ($[H^+] = 1.29$ M, $[H_2O] = 55$ M, $[MA] = 0.1$ M). Water is explicitly taken into account to comply with the GEPASI input format.

Test of the GaF-MA Model. The validity of the model was tested using the experimental rate constants in Table 1 for the following conditions at 20 °C: $[H^+] = 1.29$ M, $[MA]_0 = 0$ M, $[Ce^{4+}]_0 = 5 \times 10^{-4}$ M, $0.016\ M \leq [BrMA]_0 \leq 0.050$ M, $[BrO_3^-]_0 = 0.05$ M. The shape of the oscillations and their period (e.g., $T_2 = 500$ s for $[BrMA]_0 = 0.05$ M, and $T_2 = 650$ s for $[BrMA]_0 = 0.02$ M) are in satisfactory agreement with experimental observations.[19] Note that, as expected for the pure BrMA conditions above, R35a and R35b involving BrO_2MA play no role here. Under similar conditions but with $[BrMA]_0 = 0$ M, $[BrO_3^-]_0 = 0.1$ M, and $[Ce^{4+}]_0 = 10^{-4}$ M and [MA] =

0.1 M, or $[Ce^{4+}]_0 = 10^{-3}$ M and [MA] = 0.8 M, the simulations give a very long induction period without oscillations for $t \leq$ 3000 s. If the reactions R35a and R35b (or only R35b) are eliminated, one obtains oscillations (T = 346 s) without an induction period in the first case. This is, however, not what is observed experimentally.[24,25]

Under the conditions of our experiments ([MA] = 0.1 M, $[Br^-]_0 = 0.02$ M, $[BrO_3^-]_0 = 0.07$ M, $[Ce^{4+}]_0 = 0.488$ mM, and $[H^+] = 1.29$ M) the simulations give a long induction period without oscillations. Removing R35a and R35b also yields oscillations without an induction period as observed experimentally but with a period ($T_2 \cong 346$ s) that is about 5 times longer than observed ($T_2 \cong 76$ s). The amplitude of the oscillations is about 1.5 times larger than expected, but the shape of the oscillations (rapid autocatalysis and slow oxidation step) is in good agreement with the experimental results. At low catalyst concentrations, the agreement gets progressively worse; e.g., for $[Ce^{4+}]_0 = 0.049$ mM the calculated period is about 9 times too long and the shape of the oscillations is very different from the observed one.

When the GaF-MA model is used to simulate the data obtained under anaerobic conditions by Wang et al.[6] (see Figures 1a and 2a in their work), one obtains—but only after removal of R35b—oscillations with 15 periods between 4000 and 6000 s rather than the 31 periods observed experimentally. The shape of the oscillations and their regularity are, however, much improved compared to the original Wang model[6] (see also Figure 9).

Clearly, the GaF-MA model does not yet cover the full complexity of the $MA/BrO_3^-/Ce^{4+}$ system, but the results above and those of other simulations suggested that some progress could be achieved toward a qualitative understanding of the oxygen effect by making limited modifications.

GaF-MA-N Model. The most important modifications made to the GaF-MA model to investigate the oxygen effect are the removal of reactions R35a and R35b from the model in order to obtain oscillations and the addition of the set of reactions involving peroxymalonyl radicals ($MAOO^\bullet$), which occur during the aerobic oxidation[5] of MA by Ce^{4+}, i.e., the N reactions in Table 1 (R35−R39, R28, and R17 but not the corresponding reverse reaction R18). The resulting GaF-MA-N model thus contains 39 reactions involving 31 dynamic variables of which three are again kept constant ($[H_2O]$, $[H^+]$, [MA] = 0.1 M). The optimization steps in the simulations below were made using a somewhat lower value of k_{16} than the experimental one.[9−11] A somewhat higher value should have been used to take into account the effect of the slightly lower acidity[17] in our experiments (0.9 M H_2SO_4), but this would not have improved matters but required an increase of the value of k_{19} to 0.5 M^{-1} s^{-1} to obtain the same results.

The N Reactions. The behavior of the N reactions and in particular the abrupt drop in $MAOO^\bullet$ concentration as oxygen is consumed were first studied separately. The value[5] of k_{17} of 0.3 M^{-1} s^{-1} leads to a clear drop in the peroxymalonyl radical concentration for an initial oxygen concentration $[O_2]_0$ around 4.0×10^{-5} M and initial cerium concentrations $[Ce^{4+}]_0$ below 0.2 mM (i.e., corresponding to a biphasic behavior). This drop in peroxymalonyl radical concentration occurs only over a narrow range of $[Ce^{4+}]_0/[O_2]_0$ ratios. In fact, the time course of the $MAOO^\bullet$ concentration evolves from a curve with an initial sharp peak at low $[Ce^{4+}]_0/[O_2]_0$ ratios to one with an increasingly broad plateau and finally a smooth decay at high ratios.

A simple sensitivity analysis with fixed $[Ce^{4+}]_0 = 0.03$ mM and $[O_2]_0 = 4.0 \times 10^{-5}$ M of each of the seven rate constants of the N reactions indicates that the order of importance of the essential reactions is R17, R38, R36, R35, whereas reactions R37, R39, and R28 are of decreasing importance. Lower values of k_{17} or higher values of k_{35} are very favorable to obtain a drop. The latter becomes a peak for higher k_{36} or lower k_{38}, and a smooth decay at lower k_{36}.

With the isolated set of N reactions the malonyl radical concentration displays a transient peak in the presence of oxygen, whereas the oxygen and Ce^{4+} concentrations both decay smoothly.

Optimization and Test of the GaF-MA-N Model. Simple iterative optimization of the GaF-MA-N model with $[Ce^{4+}]_0 =$ 0.02 mM, starting from $[H^+] = 1$ M, $[O_2]_0 = 4.0 \times 10^{-5}$ M, and the experimental value of $k_{19} = 0.09$ M^{-1} s^{-1} and $k_{17} =$ 0.3 M^{-1} s^{-1}, led to the final values of $[H^+] = 1.35$ M, $[O_2]_0 =$ 2.0×10^{-4} M, $k_{19} = 0.4$ M^{-1} s^{-1}, and $k_{17} = 0.23$ M^{-1} s^{-1}. The increase in $[H^+]$ compared to the value at 20 °C (1.29 M) only slightly reduces the period of the oscillations by accelerating the oxidation. The value of k_{19}, which is crucial for all BZ models, was increased to 0.4 M to obtain a phase-1-like behavior and to increase the frequency of the oscillator. This increase cannot be justified by the difference between the temperatures at which the experimental data have been obtained (30 °C) and the rate constant measured (20 °C). Indeed, if the experimental value of k_{17} is doubled to simulate the effect of temperature, the value of k_{19} must also be increased to about 1.0 M^{-1} s^{-1} to still obtain similar results. It should be noted, however, that some authors have increased this value up to 30 M^{-1} s^{-1} to model their observations.[7,9−11] If the stoichiometry of R33 is changed[26] to produce $2Br^-$ to simulate the increased bromide production under aerobic conditions, the optimal value of k_{19} in the simulations is only a factor of 2 larger than the experimental value.

As illustrated in Figure 8, the GaF-MA-N model only reproduces a phase-1-like structure but in a very narrow range of initial cerium concentrations around 0.02 mM where there are no oscillations in the experimental data. At lower catalyst concentrations, this phase-1-like structure becomes, in contrast with the experimental results, an induction period without oscillations. Phase 1 oscillations with a larger amplitude and a clearly longer period than in phase 2 as observed experimentally could not be reproduced despite a large number of simulation runs. The shape of the phase 2 oscillations and its evolution with the initial cerium concentration is in qualitative agreement with the observation in the range ~0.04−0.8 mM. The value of T_2 for $[Ce^{4+}]_0 = 0.488$ mM is about 3 times too large, whereas the average Ce^{4+} concentration (DC_2) and the amplitude excursions ($2AC_2$) are about 1.5−2 times larger than the experimental ones. The results for phase 2 are still significantly better than those obtained with the GaF-MA model, especially at lower catalyst concentrations, as illustrated in Figure 8.

The GaF-MA-N model predicts a smooth decay of the oxygen concentration with small periodic steps, characteristic of irreversible reactions, rather than oscillations, although oscillations have been reported for the signal of an oxygen electrode, albeit under different conditions.[6]

When the modified value of k_{19} is introduced in the GaF-MA model (without R35b) with[5] $k_{28} = 4.2 \times 10^8$ M^{-1} s^- and $[H^+] = 1.35$ M, the results of Wang et al.[6] for the anaerobic cerium oscillator are better reproduced than by the original Oregonator or by the GaF-MA model with the experimental value of k_{19} above, as illustrated by comparison of the results in Figure 9 (top) with the experimental data in Figures 1a and 2a in their work. The shape of the oscillations and their

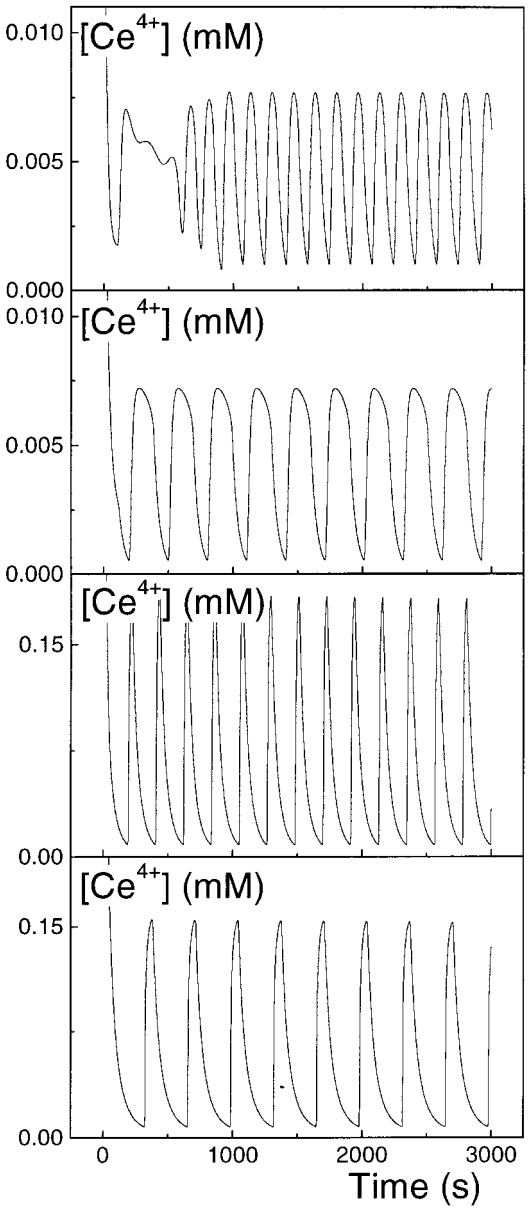

Figure 8. Comparison of the results (Ce^{4+} concentrations) of the simulations obtained with the GaF-MA-N model (top curve) and the GaF-MA model (curve 2 from top) for an initial cerium concentration $[Ce^{4+}]_0 = 0.020$ mM. Curves 3 (GaF-MA-N) and 4 (GaF-MA) from the top give a similar comparison for $[Ce^{4+}]_0 = 0.488$ mM. The concentrations of H_2O (55 M), MA (0.1 M), and H^+ (1.35 M) were kept constant. Initial concentrations were $[Br^-]_0 = 0.02$ M, $[BrO_3^-]_0 = 0.07$ M, and, for GaF-MA-N, also $[O_2]_0 = 2.0 \times 10^{-4}$ M.

regularity are considerably improved, and the duration of the simulated oscillations as well as the period are closer to the experimental ones (31 periods between 4000 and 6000 s in the experimental data against 23 periods in the present simulation, 15 in the GaF-MA model, and only 18 in the original Oregonator model[6]) without the need for the unrealistic cerium concentrations of the latter model.

To model the transfer of oxygen from the gas phase to the solution under the aerobic conditions of Wang et al.,[6] an additional reaction (R40) with $k_{40} = 8.33 \times 10^{-5}$ s^{-1} and $[O_{2gas}]$ constant was introduced. When the parameters ($[O_{2gas}]$, k_{40}, $[H^+]$, $[Ce^{4+}]_0$, k_{35}, k_{36}, k_{37}) are changed one at a time for conditions close to those of Wang et al.[6] ($[Br^-]_0 = 0$ M, $[BrO_3^-]_0 = 0.0467$ M, [MA] = 0.444 M, $[Ce^{4+}]_0 = 2.2$ mM, $[O_{2gas}]$ around 4.3 mM or 10.5% (with [MA] = 0.444 M, $[H_2O]$ = 55 M, and

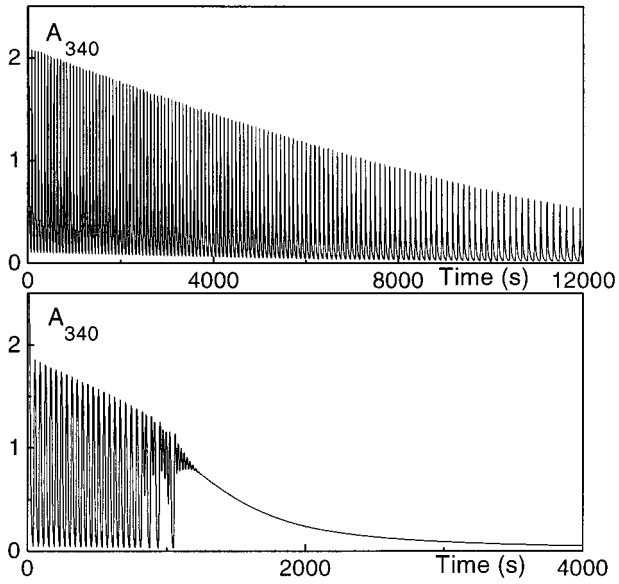

Figure 9. (Top) GaF-MA model gives a better agreement with the anaerobic data in Wang et al.[6] than the original model ($[Ce^{4+}]_0 = 2.2$ mM). The absorbance at 340 nm (A_{340}) was calculated assuming $\epsilon_{340}^{Ce^{4+}} = 5098$ M^{-1} cm^{-1} and an optical path of 1 cm. This figure should be compared with Figures 1a and 2a in Wang et al.[6] (Bottom) Onset of complexity as predicted by the GaF-MA-N model enhanced with a reaction for gas-solution oxygen transfer (R40 in Table 1) to simulate the aerobic conditions in Wang et al.[6] ($[Ce^{4+}]_0 = 2.3$ mM, $[O_{2gas}] = 90$ mM, $k_{40} = 9.0 \times 10^{-5}$ s^{-1}). Other conditions were $[Br^-]_0 = 0$ M, $[BrO_3^-]_0 = 0.0467$ M. $[H_2O] = 55$ M, [MA] = 0.444 M, $[H^+] = 1.35$ M, and $[O_{2gas}]$ were kept constant.

$[H^+]$ constant around 1.35 M)), the behavior always switches from regular oscillations lasting a long time to oscillations that last briefly and end with a few groups of complex oscillations (period-4, period-8, etc.) followed by a smooth decay as illustrated in Figure 9 (bottom). With the above parameters, complex behavior appears for $[O_{2gas}]k_{40} \cong 8 \times 10^{-6}$ M s^{-1}, and additional simulations suggest that it is unlikely that conditions could be found yielding complexity over a long time interval in the simulations, although it cannot be excluded given the narrow range of parameters for which complexity could be obtained.

Simulation of the Effect of Acrylonitrile. The effect of acrylonitrile was simulated by addition of two fast reactions representing the reaction of acrylonitrile (X) with malonyl radicals (R41a) and its polymerization (R41b) and by decreasing the initial oxygen concentration in the GaF-MA-N model. The results are illustrated in Figure 10. If the initial oxygen concentration is not lowered, the rectangular induction period is followed by a smooth exponentially decaying tail before the onset of oscillations. It is plausible that addition of inhibited acrylonitrile prior to that of the catalyst would indeed reduce the effective initial oxygen concentration. Except for the pronounced increase of the induction period at high acrylonitrile concentrations, which was not observed, the main features in the simulated curves are very similar to those of the experimental ones in Figure 5.

Effect of Initially Added Bromide on the Phase 1 Oscillations. In GEPASI, perturbations can be applied to a system during its evolution by pausing the simulation at the desired instant and directly altering the value of a concentration. This feature was used to "inject" oxygen only or oxygen and bromide during the GaF-MA-N simulations. Curve B in Figure 11 illustrates the simulated effect on the BZ system of two injections of oxygen during the second phase. The decay in Ce^{4+} concentra-

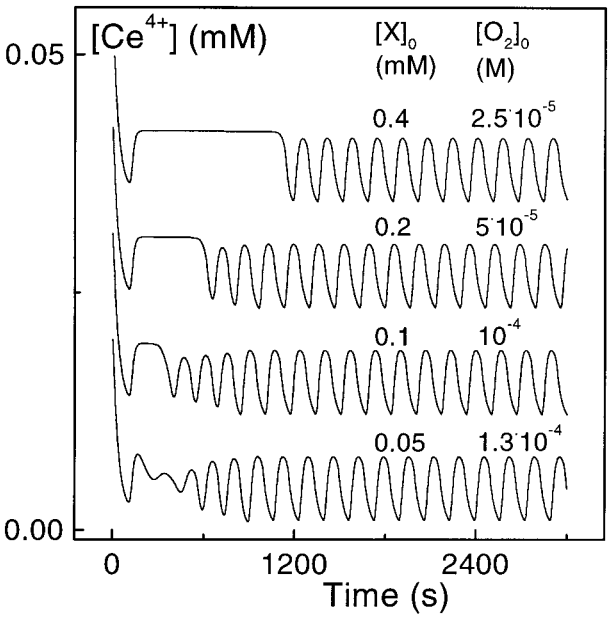

Figure 10. Simulation of the effect of acrylonitrile (X) using the GaF-MA-N model with two additional reactions (R41a and R41b in Table 1) (compare with the experimental data in Figure 6). Initial concentrations were 0.02 mM Ce^{4+}, 0.02 M Br^-, 0.07 M BrO_3^-. The concentrations of H_2O (55 M), MA (0.1 M), and H^+ (1.35 M) were kept constant.

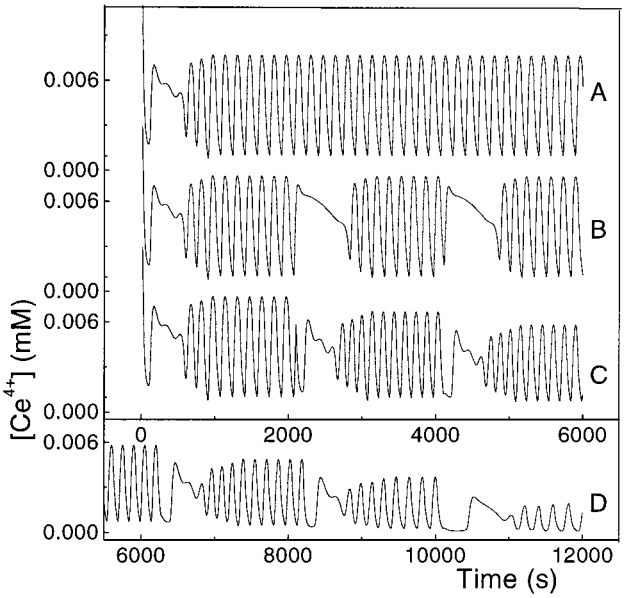

Figure 11. Simulation of the effect of oxygen and oxygen + bromide injections during phase 2: (curve A) unperturbed system; (curve B) O_2 (2.0×10^{-4} M) injected at $t = 2039.5$ s and $t = 4079.5$ s; (curve C) O_2 (2.0×10^{-4} M) and Br^- (0.02 M) injected simultaneously at $t = 2039.5$ s and $t = 4079.5$ s; (curve D) O_2 (2.0×10^{-4} M) and Br^- (0.02 M) injected simultaneously at $t = 2159.5$ s, 4079.5 s (not shown), 6239.5, 8159.5, and 10079.5 s. $[H_2O] = 55$ M, $[MA] = 0.1$ M, and $[H^+] = 1.35$ M were kept constant. $[Ce^{4+}]_0 = 0.02$ mM, $[O_2]_0 = 2.0 \times 10^{-4}$ M, $[Br^-]_0 = 0.02$ M, $[BrO_3^-]_0 = 0.07$ M.

tion is faster than in the experimental data (Figure 5, injection 2). A phase 1 without oscillations can thus be attributed to a pure oxygen effect: removal of malonyl radicals and formation of peroxymalonyl radicals.

Oscillations can be obtained if bromide is injected simultaneously with oxygen (Figure 11, curve C). The features of phase 1 are thus clearly determined by two distinct contributors: oxygen (induction period) and initially added bromide (superimposed oscillations). The drop is, however, not correctly reproduced, and the progressively increasing amplitude after the induction period is not observed experimentally.

In a series of successive simulated O_2 + bromide injections, illustrated in curve D in Figure 11, the oscillatory component dies out, whereas the induction period component is still observed. When oxygen injection during phase 1 is simulated, this phase becomes longer but the oscillations disappear (not shown). The latter effect is not observed experimentally (see Figure 5, injection 1). This discrepancy could be due to a faster decay of the initially added bromide in the simulated system than in the experimental one or to an inadequate oxygen/bromide ratio in the simulations.

Conclusions

The experimental results of the BZ reaction at low initial cerium concentrations ($[Ce^{4+}]_0 < 0.3$ mM) in the absence of oxygen (i.e., in phase 2) provide a stringent test for any proposed mechanism because the period of the oscillator changes rapidly with initial catalyst concentration. The higher average Ce^{4+} concentrations, higher amplitudes, and longer oscillation periods in phase 1 are consistent with the effect of the initial cerium concentration on the amplitude and period in phase 2.

The experimental evidence strongly suggests that the drop in average Ce^{4+} concentration in the presence of oxygen is a property of the MA/Ce^{4+} or $Ce^{3+}/BrO_3^-/H_2SO_4$ system involving malonyl radicals, which occurs only in a very narrow range of concentrations. It should be noted that although break points were observed in the oxidation of malonic acid by Ce^{4+} very early on,[27] experimental evidence for the effect of oxygen on the oxidation of small organic acids by Ce^{4+} is still very scarce.[5,28]

The simulations using models with close to experimental rate constants qualitatively reproduce some of the features of the cerium oscillator at low catalyst concentrations in the presence and absence of oxygen as well as of the perturbations due to acrylonitrile. They also give a significantly better agreement with some of the recently published data on the BZ reaction than some of the original models.[6]

The failure to reproduce the enhancement of Ce^{4+} concentration in phase 1 and the experimental data in the absence of initially added bromide (with or without $AgNO_3$) suggests that the effect of oxygen on the mechanism of oxidation of malonic acid by Ce^{4+} in acidic medium[5] is significantly affected by the presence of bromate. This would require further investigation.

The observations above and the simulations using the GEPASI program[16] provide an interesting extension to the popular laboratory manual of Pojman et al.[12]

Acknowledgment. A.-M. P. is grateful to the EMBL for a predoctoral fellowship. The authors thank Prof. R. J. Field for useful suggestions and Dr. P. Mendes for a copy of GEPASI.

References and Notes

(1) Zhabotinsky, A. M. *Dokl. Akad. Nauk. SSSR* **1964**, *157*, 392.
(2) Field, R. J.; Körös, E.; Noyes, R. M. *J. Am. Chem. Soc.* **1972**, *94*, 8649.
(3) Barkin, S.; Bixon, M.; Noyes, R. M.; Bar-Eli, K. *Int. J. Chem. Kinet.* **1978**, *10*, 619.
(4) Bar-Eli, K.; Haddad, S. *J. Phys. Chem.* **1979**, *83*, 2952.
(5) Neumann, B.; Müller, S. C.; Hauser, M. J. B.; Steinbock, O.; Simoyi, R. H.; Dalal, N. S. *J. Am. Chem. Soc.* **1995**, *117*, 6372.
(6) Wang, J.; Hynne, F.; Sörensen, P. G.; Nielsen, K. *J. Phys. Chem.* **1996**, *100*, 17593.
(7) Treindl, L.; Ruoff, P.; Kvernberg, P. O. *J. Phys. Chem. A* **1997**, *101*, 4606.
(8) Gao, Y.; Försterling, H.-D. *J. Phys. Chem.* **1995,** *99*, 8638.

(9) Györgyi, L.; Turanyi, T.; Field, R. J. *J. Phys. Chem.* **1990**, *94*, 7162.
(10) Györgyi, L.; Field, R. J. *J. Phys. Chem.* **1991**, *95*, 6594.
(11) Györgyi, L.; Rempe, S. L.; Field, R. J. *J. Phys. Chem.* **1991**, *95*, 3159.
(12) Pojman J. A.; Craven, R.; Leard, D. C. *J. Chem. Educ*. **1994**, *71*, 84.
(13) Försterling, H. D.; Schreiber, H.; Zittlau, W. *Z. Naturforsch.* **1978**, *33a*, 1552.
(14) Noszticzius, Z.; McCormick, W. D.; Swinney, H. L. *J. Phys. Chem.* **1987**, *91*, 5129.
(15) Pojman, J. A.; Leard, D. C.; West, W. *J. Am. Chem. Soc*. **1992**, *114*, 8298.
(16) Mendes, P. *Comput. Appl. Biosci.* **1993**, *9*, 563.
(17) Försterling, H.-D.; Varga, M. *J. Phys. Chem.* **1993**, *97*, 7932.
(18) Field, R. J.; Försterling, H.-D. *J. Phys. Chem.* **1986**, *90*, 5400.
(19) Yan, S.; Försterling, H.-D. Manuscript in preparation.
(20) Sirimungkala, A. Ph.D. Thesis, Philipps-Universität Marburg, Germany, 1996.
(21) Sirimungkala, A.; Försterling, H.-D.; Noszticzius, Z. *J. Phys. Chem.* **1996**, *100*, 3051.
(22) Försterling, H.-D.; Stuk, L. *J. Phys. Chem.* **1991**, *95*, 7320.
(23) Oslonovitch, J.; Försterling, H.-D.; Wittmann, M.; Noszticzius, Z. *J. Phys. Chem.* **1998**, *A102*, 922.
(24) Murányi, S.; Försterling, H.-D. *Z. Naturforsch.* **1990**, *45a*, 135.
(25) Försterling, H.-D.; Murányi, S. *Z. Naturforsch.* **1990**, *45a*, 1259.
(26) Försterling, H.-D.; Stuk, L.; Barr, A.; McCormick, W. D. *J. Phys. Chem.* **1993**, *97*, 2623.
(27) Jwo, J.-J.; Noyes, R. M. *J. Am. Chem. Soc.* **1975**, *97*, 5422.
(28) Neumann, B.; Steinbock, O.; Müller, St. C.; Dalal, N. S. *J. Phys. Chem.* **1996**, *100*, 12342.
(29) Försterling, H.-D.; Pachl, R.; Schreiber, H. *Z. Naturforsch.* **1987**, *42a*, 963.
(30) Försterling, H.-D.; Idstein, H.; Pachl, R.; Schreiber, H. *Z. Naturforsch.* **1984**, *39a*, 993.
(31) Sirimungkala, A.; Försterling, H.-D.; Dlask, V.; Field, R. J. *J. Phys. Chem.*, in press.
(32) Gao, Y.; Försterling, H.-D.; Noszticzius, Z.; Meyer, B. *J. Phys. Chem.* **1994**, *98*, 8377.